2022

Quasi 1D Modelling of Conical Rotary Compressors

Yang Lu

Hoang Khoi

David Noake

Nicol Low

Quasi 1D modelling of conical rotary compressors

Yang LU*, Ken HOANG, David NOAKE and Nicol LOW

Vert Techanology,
Edinburgh, Scotland
Yang.lu@vertrotors.com
ken.hoang@vertrotors.com
david.noake@vertrotors.com
nicol.low@vertrotors.com

* Corresponding Author

ABSTRACT

The Conical Rotary Compressor (CRC) is a versatile Positive Displacement Machine (PDM) consisting of one inner conical screw rotor rotating inside an outer conical screw rotor, which has various applications in heat pump, refrigeration, compression and vacuum fields. Quasi-steady modelling has been successfully implemented on piston compressors, scroll compressors and twin-screw compressors to optimize performance and compressor design. This study is intended to develop the mathematical model to simulate the quasi-steady performance based on the geometrical and working characteristics of conical rotary compressor. The control volume of the CRC is firstly calculated. Secondly, based on the assumptions for the analysis of the control volume, the conservation equations of mass and energy, state equation with considering of leakage are solved using adaptive Runge-Kutta method. Finally, the volume flow rate and specific power of air conical rotary compressor are calculated and compared with experimental results to improve and validate the model. Based on this study, the working performance, rotor profile, size and cost of conical rotary compressors can be optimized at the design stage.

1. INTRODUCTION

Conical rotary compressor is an innovative positive displacement machine which consists of one inner rotor rotating inside an outer rotor. CRC machine has features of internal meshing, variable pitch and profile which offer several advantages including higher built-in volume ratio, lower relative velocity and gradual pressure increasing so that higher-pressure ratio operation could be achieved. Therefore, the machine is suitable for air conditioning, heat pump application. PDM such as gerotor (Read et al., 2019), scroll compressors (Morishita et al., 1984), (Chen, Halm, Groll, et al., 2002) (Chen, Halm, Braun, et al., 2002)single screw compressors (Bell et al., 2020) and twin-screw compressors (Hanjalic & Stosic, 1997; Stosic & Hanjalic, 1997) have been studied for decades for profile design, quasi 1D thermodynamic calculation and 3D CFD simulation. Commercial software package such as SCORPATH and open-source software package such as PDsim (Bell et al., 2020) have been developed to calculate the geometrical characteristics and thermodynamic performance. However, very few research on the CRC machine. The thermodynamic model was developed for PDM could be employed in CRC machine. In this paper, the geometry such as chamber volume and leakage paths of base line of the commercial Vert CRC.60 machine are analyzed based on the developed program and the thermal dynamic properties are calculated and compared with experimental results.

2. GEOMETRY

The main parts of CRC.60 are inner rotor, outer rotor, housing and end cover. The CNC machined rotors and schematic rotor geometry are shown in Figure 1. The motor directly connects with inner rotor which drives outer rotor. Both rotors rotates in same direction along fixed axis.

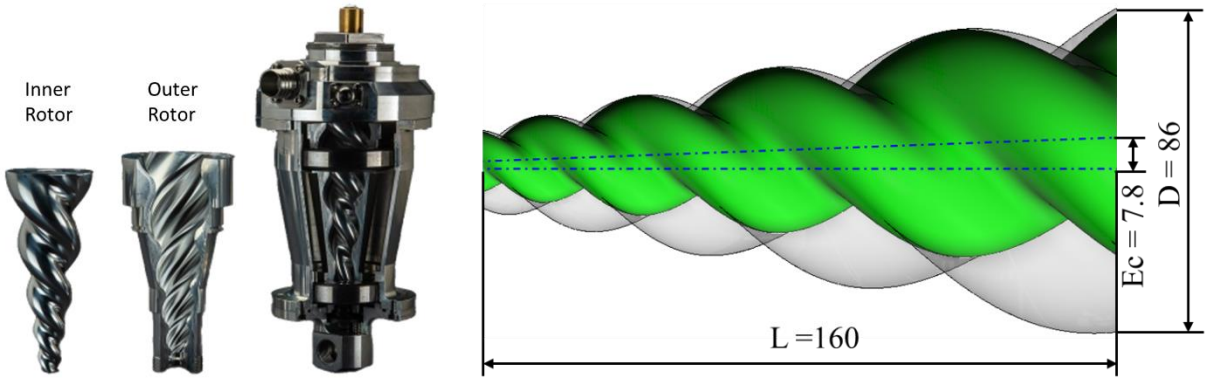

Figure 1: CRC.60 3D model

The geometric parameters are listed in Table 1. The rotor length of inner rotor and outer rotor is 160 mm. The maximum center distance and outer rotor diameter are 7.8 mm and 86 mm individually which are decreasing along rotor. The suction volume is 30 cc which is achieved when the chamber disconnects with suction chamber. It is worth noticing that the maximum chamber volume is greater than 30 cc.

Table 1: CRC.60 Geometric parameters

Parameters	Unit	Value	Parameters	Value
Ec	[mm]	7.8	Vi	4.6
V_suc	[cc]	30	Z1/Z2	3/2
L	[mm]	160	No. wrap 1/2	1.52/2.28
D1	[mm]	86	Di	4.3

CRC.60 is a 3 by 2 number of lobe combination compressor (N32). The 3 by 2 and 4 by 3 lobe combination rotor profiles are shown in Figure 1. The rotor profiles are generated with cutting tool method, as described in the Vert patent.

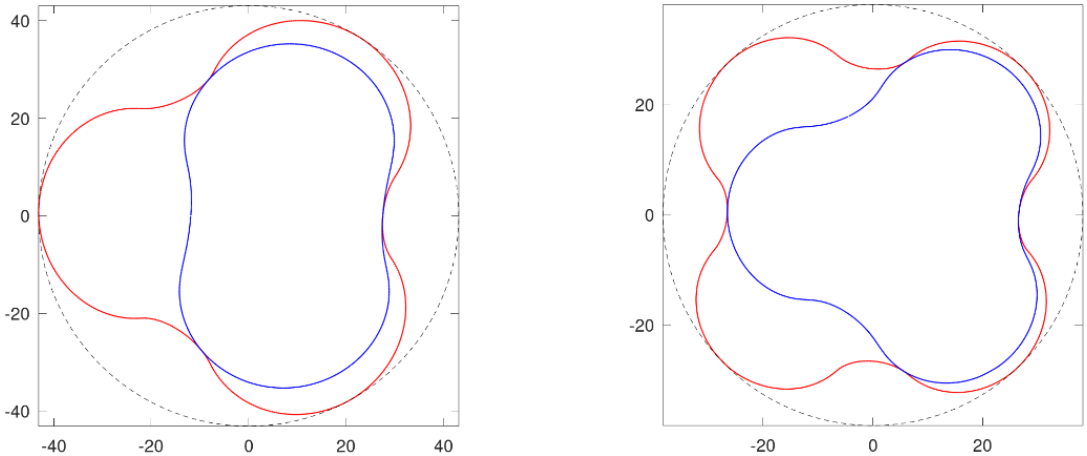

Figure 2: Rotor profile

2.1 Chamber Volume

Based on the wrap angle of N32, outer rotor rotational angle range is from 0 to 907 degree. Maximum chamber volume is achieved at 220-degree and suction end chamber volume is obtained at 360-degree when suction chamber

disconnected with suction chamber. The discharge chamber volume is achieved at 547-degree. It takes 360-degree to finish discharge process. The working process of CRC machine is listed in Table 2.

Table 2 Working process of CRC machine

Process	Degree	Comment
Suction	[0, 360]	Chamber volume Vc increases from 0 to maximum at 180 degree and closed from suction at 360-degree.
Internal compression	[360,547]	Chamber volume continues decrease leading to internal compression.
Discharge	[547 907]	Chamber volume decreases to 0 after 360-degree.

Chamber volume is calculated from the in-house software VertSim and illustrated in Figure 3. Rotation angle is based on outer rotor. With the rotation of the outer rotor, the chamber volume between inner rotor and outer rotor starts to increase. Because the suction port is not designed, the chamber is still connected with suction chamber when the chamber volume reaches to maximum. The suction process finishes at 360 degree rotational angle. Likewise, the discharge process finishes at 360 degree before the end of the discharge. The diagram of volume and rotational angle could provide the reference for the design of suction and discharge ports.

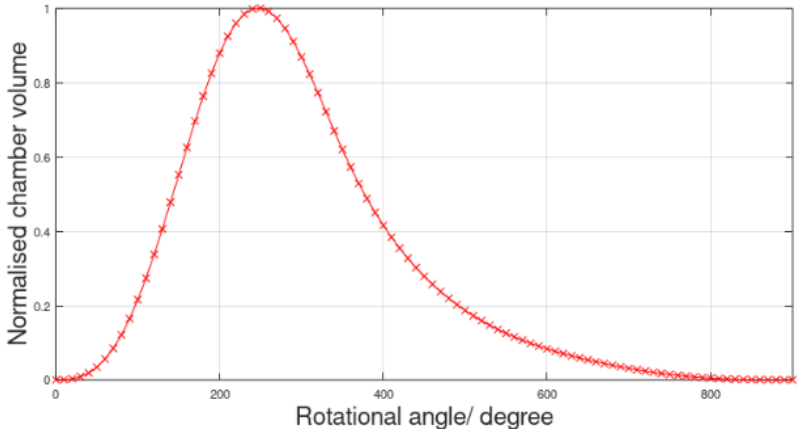

Figure 3: Chamber volume changing with rotational angle

2.2 Sealing line length

There are two different type of leakage paths which are axial and radial gaps existing between inner and outer rotors in CRC machine. Leakage paths are demonstrated in
Figure 4. C1 is the control chamber. It takes 360-degree rotation to form a fully closed chamber, so chamber C1 can simultaneously connect to maximum 6 chambers which are upstream chambers C2, C11 and C31 and downstream chambers C22, C12 and C3. Chamber C1 will leak in or out from adjacent chambers. Normally, downstream chambers will leak into chamber C1 and upstream chambers will get leakage from chamber C1.

<table>
<tr><td rowspan="3">Suction</td><td colspan="2">C2 - Radial</td><td colspan="2">C22 – Radial</td><td rowspan="3">Discharge</td></tr>
<tr><td>C11 – Axial</td><td>C1</td><td colspan="2">C12 – Axial</td></tr>
<tr><td colspan="2">C31 – Radial</td><td colspan="2">C3 - Radial</td></tr>
</table>

Figure 4 Leakage paths

2.2.1 Axial leakage: There are a maximum of two axial leakage paths for the control chamber. YZ cross section of CRC rotors is shown in
Figure **5** (a) to visualize the leakage paths. In this relative position, chamber C11 and C12 are axially adjacent to chamber C1. Chamber C11 connected to suction chamber and C12 connected to discharge chamber. It is assumed

that the axial leakage only exists when chamber C11 and C12 disconnected with suction and discharge chamber. There is 360-degree rotation angle difference between chamber C1 and chamber C11 and chamber C12.

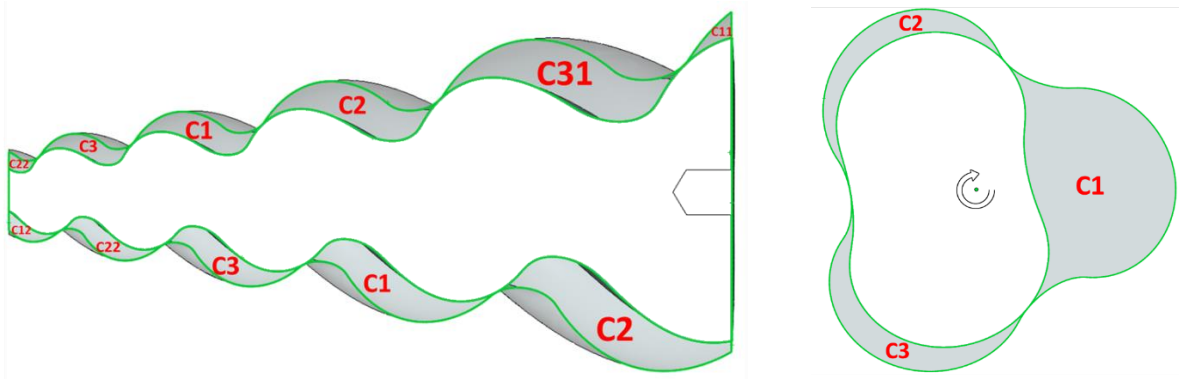

YZ cross section (a) XY cross section

Figure 5: Rotor cross sections to show leakage paths

The variation of leakage length of C11 and C12 with outer rotor rotational angle is shown in Figure **6** (a). Leakage length of C11 is only calculated when the chamber C1 is disconnected with suction chamber and discharge chamber, which is the reason that leakage length is 0 in the range of [0 360] and range [547 907].

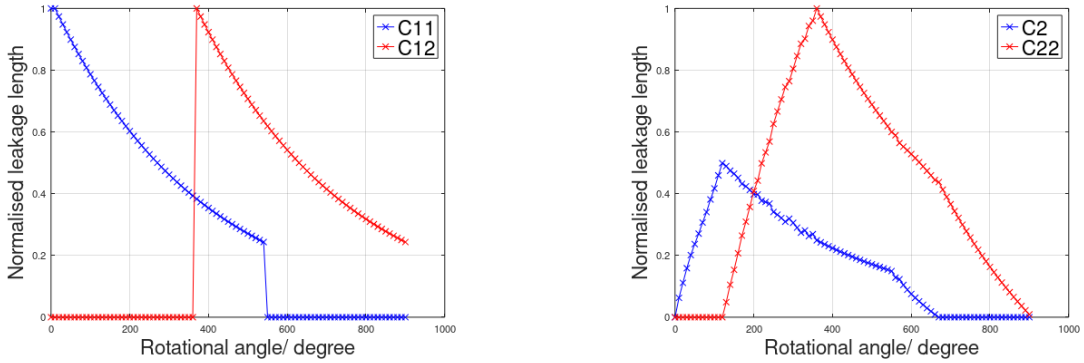

Axial leakage length Radial leakage length

Figure 6: Chamber volume changing with rotational angle

2.2.2 Radial leakage: Radial leakage is relatively more complex. There are four radial leakage paths. XY cross section in Figure **5** (b) shows two radial leakage paths. Chamber C2 and C3 are radially adjacent to chamber C1. Chamber C2 is 120-degree lag to chamber C1 while chamber C3 is 120-degree advance to chamber C1. If XY cross section was taken in different axial position, chamber C3 could be replaced by chamber C22 and chamber C2 could be replaced by chamber C31. Chamber C22 and C31 are radially adjacent to chamber C1. Chamber C22 is 240-degree advance to chamber C1 while chamber C31 is 240-degree lag to chamber C1. The variation of radial leakage paths of C2 and C22 with outer rotor rotational angle is shown in Figure **6** (b). The whole leakage length is divided to two segments which are the gaps between downstream and upstream chambers. Radial leakage paths of C3 and C31 have same patten and can be obtained by translation of C2 and C22.

3. MATHEMATICAL MODEL

The mathematical model of simulating working process of CRC is based on the changing chamber volume and considering effect of leakage, oil-injection and heat transfer. A set of differential equations can be built based on law of conservation of energy and mass.

3.1 Assumptions

The working process of CRC was simulated using quasi-one-dimensional thermodynamic model. In order to ensure efficient computation, the model has some assumptions. These are as follows:

- The suction and discharge chambers are infinite. In this case, pressure pulsations can be ignored.
- The density, velocity, pressure and temperature are homogeneous in control chamber.
- The fluid flow is assumed to be quasi-one-dimensional.
- The kinetic energy of the fluid is neglected in comparison with its internal energy.
- The flow of the gas is assumed to be isentropic, while the leakage flow is regarded as adiabatic.

3.2 Basic equations

According to the first law of thermodynamics, the conservation of internal energy equation can be written as equation (1):

$$d(mu) = dE_i - dE_o - dQ + dW \tag{1}$$

Then:

$$d(mu) = \sum dm_i \left(h_i + \frac{v_i^2}{2} + z_i g\right) - \sum dm_o \left(h_o + \frac{v_o^2}{2} + z_o g\right) - \sum dQ + dW \tag{2}$$

Ignore the kinetic energy and potential energy and consider $d\phi = \omega dt$, $u = h - pv$, $v = V_c/m$ ($V_c$is the chamber volume) and the continuity equation $dm = dm_i - dm_o$ and $dW = -pdV_c$, equation (3) could be derived.

$$\frac{dp}{d\varphi} = \frac{1}{v}\left[\left(\frac{\partial h}{\partial v}\right)_T \frac{dv}{d\varphi} + \left(\frac{\partial h}{\partial T}\right)_v \frac{dT}{d\varphi}\right] - \frac{1}{V_c}\left[\sum \frac{dm_i}{d\varphi}(h_i - h) - \frac{dQ}{d\varphi}\right] \tag{3}$$

According to the equation of state for ideal gases：

$$\frac{dp}{d\varphi} = \left(\frac{\partial p}{\partial v}\right)_T \frac{dv}{d\varphi} + \left(\frac{\partial p}{\partial T}\right)_v \frac{dT}{d\varphi} \tag{4}$$

Solve the $\frac{dT}{d\varphi}$from the equation (4) and substituting to equation (3), the changing of the pressure in chamber with the time can be derived as equation (5).

$$\frac{dp}{d\varphi} = \frac{\frac{1}{v}\left[\left(\frac{\partial h}{\partial v}\right)_T - \frac{(\partial h/\partial T)_v (\partial p/\partial v)_T}{(\partial p/\partial T)_v}\right]\frac{dv}{d\varphi} - \frac{1}{V_c}\left[\sum \frac{dm_i}{d\varphi}(h_i - h) - \frac{dQ}{d\varphi}\right]}{1 - \frac{1}{v}\frac{(\partial h/\partial T)_v}{(\partial p/\partial T)_v}} \tag{5}$$

Substitute equation (4) to equation (5), the differential form of temperature in chamber can be derived as equation (6).

$$\frac{dT}{d\varphi}=\frac{\left[\frac{1}{v}\left(\frac{\partial h}{\partial v}\right)_T-\left(\frac{\partial p}{\partial v}\right)_T\right]\frac{dv}{d\varphi}-\frac{1}{V_c}\left[\sum\frac{dm_i}{d\varphi}(h_i-h)-\frac{dQ}{d\varphi}\right]}{\left(\frac{\partial p}{\partial T}\right)_v-\frac{1}{v}\left(\frac{\partial h}{\partial T}\right)_v} \tag{6}$$

Equation (5) and equation (6) are basic functions which describe pressure and temperature variation with rotational angle. To solve the differential equations, more supplement equations need to be added.

3.2.1 Leakage model: The leakage model is the isentropic compressible nozzle flow model.

$$\text{When } \left(\frac{2}{k+1}\right)^{\frac{k}{k-1}}\le\frac{p_2}{p_1}\le 1:\ \ \frac{dm}{d\phi}=\frac{CAp_1}{\omega}\sqrt{\frac{2k}{(k-1)RT_1}\left(\left(\frac{p_2}{p_1}\right)^{\frac{2}{k}}+\left(\frac{p_2}{p_1}\right)^{\frac{k+1}{k}}\right)} \tag{7}$$

$$\text{When } 0\le\frac{p_2}{p_1}\le\left(\frac{2}{k+1}\right)^{\frac{k}{k-1}}:\ \ \frac{dm}{d\phi}=\frac{CAp_1}{\omega}\sqrt{\frac{k}{(k-1)R}\left(\frac{2}{k+1}\right)^{\frac{k+1}{k-1}}} \tag{8}$$

In the equation, p_1 and p_2 are high pressure and low pressure with the unit Pa and the T_1 is the high-pressure side temperature with unit K. The A is the total leakage area with the unit m^2. The C is the leakage coefficient which can be obtained by the experiments.

3.2.2 Solving equation: Based on built mathematical model, pressure and temperature in control chamber and volume flow rate, indicated power can be calculated. In general, Runge-kutta method is used to solve the differential equation. In the beginning of calculation, no leakage adiabatic process is calculated to get gas state of front and back chamber. Then, leakage flow is calculated based on pressure difference between front and back chamber. Pressure, temperature and mass are compared with last calculation until the difference between two steps satisfied with given precision. After calculation of working process, Volumatic flow rate, indicated power and Volumatic efficiency can be calculated.

3. RESULTS

The gap distance is 0.005 mm which is uniform for all the leakage paths. The leakage coefficient is chosen based on the experiment results. The working conditions are listed in Table 3. The above chamber volume, axial leakage and mathematical model are used for the thermal dynamic calculation. The heat transfer and oil-injection will be considered in the later calculation.

Table 3: Working conditions and fluid properties

Parameters	Unit	Value	Air Properties	Unit	Value
n 1/2	$[rpm]$	2000/3000	Molar Mass	$[g\ /mol]$	28.97
P_suc	$[bar]$	1	Specific Heat Capacity	$[J/(kg\ K)]$	1006.43
P_dis	$[bar]$	8	Dynamic Viscosity	$[Pa\ s]$	1.72x10-5
T_suc	$[K]$	300	Thermal Conductivity	$[W/(m\ K)]$	0.0242
T_wall	$[K]$	300	Density	$[kg/m3]$	1.225

The pressure diagram is shown in
Figure **7**. Ideal process is compared with the model considering axial and radial leakage paths. Over-compression can be observed because of leakage.

Figure **7** (b) shows the pressure variation with chamber volume. There is a process that the pressure keeps constant with chamber volume decreeing. That is because the control chamber is still connected with suction chamber. Technologically, compression process starts from the chamber volume reach maximum. There is no suction port of the base line of Vert CRC.60 machine, which result in the compression process starts when the chamber volume is decreasing. A suction port plate could be positioned to disconnect the chamber when volume reach maximum, then the volume flow rate could increase.

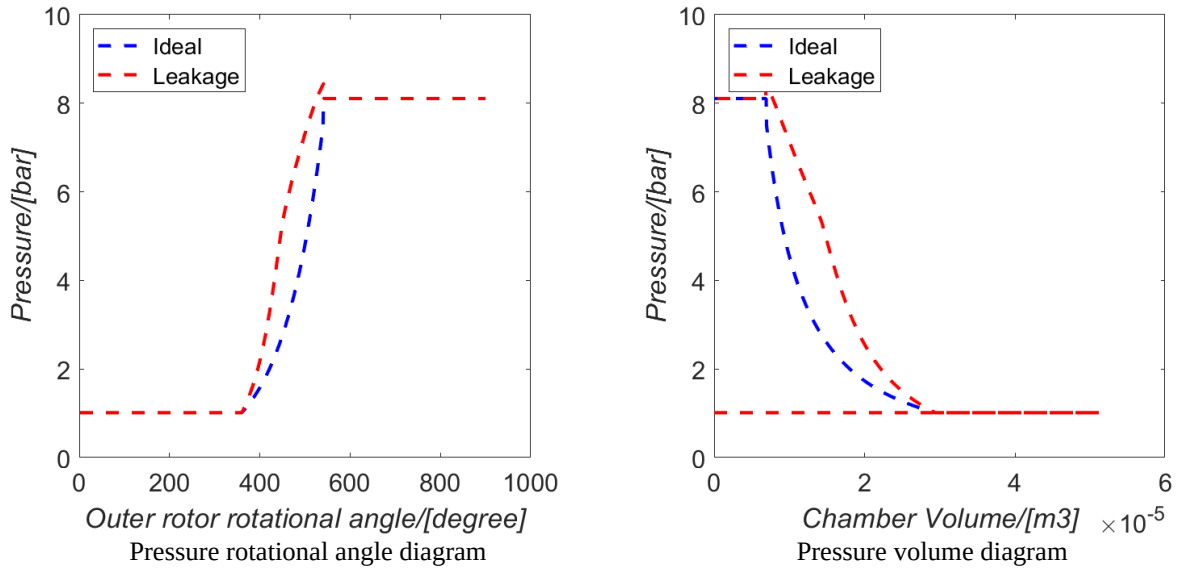

Figure 7: Pressure diagram

The test rig to measure the performance of the compressor is shown in
Figure **8**. Discharge pressure is regulated before oil separator. Inlet volume flow rate, torque, oil temperature and measured and recoded. Inlet volume flow rate and power are measured to compare with simulation results.

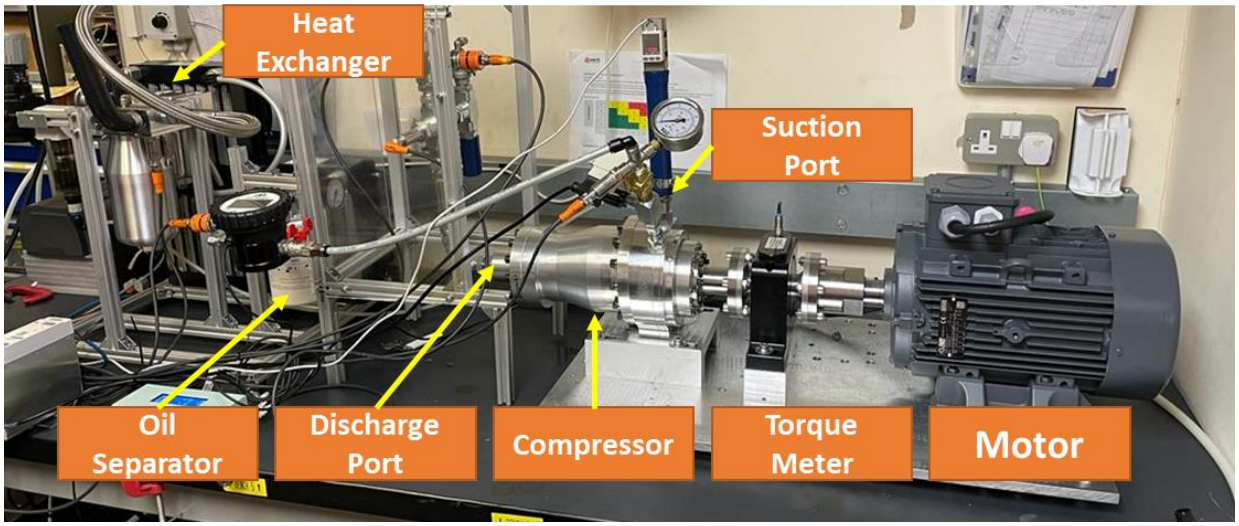

Figure 8: Test rig

The volume flow rate and power were calculated and compared with experimental results in Table 4. The inlet volume flow rate is 8% lower than experimental result. The reason is that the simulation does not consider the changing of

the leakage gap. The power difference is because of indicated power (without considering mechanical losses) for the simulation while the shaft power for the experiment.

Table 4: Comparison of volume flow rate and power

Parameters	Unit	Simulation	Experiment
Inlet volume flow rate	$[L/min]$	154.5	168.00
Indicated Power/Shaft power	$[kW]$	1.14	1.48
Volumetric efficiency	%	87.7	92.1

3. Conclusions

In this paper, the geometry of CRC machine is analysed and the mathematical model for thermodynamic calculation of CRC machine was developed by considering leakage and heat transfer. The simulation results are compared with experimental results and good agreement is achieved by using the developed chamber model. Based on this study, the working performance of different rotor profile, size and cost of conical rotary compressors can be optimized at the design stage.

NOMENCLATURE

Ec	Distance between rotor axes	mm
L	Rotor length	mm
D	Diameter of rotor	mm
V	Chamber volume	cc
N	Speed	rpm
Vi	Volume index	
Di	Diameter index	

Subscript

1	Outer rotor
2	Inner rotor

REFERENCES

Bell, I. H., Ziviani, D., Lemort, V., Bradshaw, C. R., Mathison, M., Horton, W. T., Braun, J. E., & Groll, E. A. (2020). PDSim: A general quasi-steady modeling approach for positive displacement compressors and expanders. *International Journal of Refrigeration*, *110*, 310–322. https://doi.org/10.1016/j.ijrefrig.2019.09.002

Chen, Y., Halm, N. P., Braun, J. E., & Groll, E. A. (2002). Mathematical modeling of scroll compressors-part II: overall scroll compressor modeling. In *International Journal of Refrigeration* (Vol. 25). www.elsevier.com/locate/ijrefrig

Chen, Y., Halm, N. P., Groll, E. A., & Braun, J. E. (2002). Mathematical modeling of scroll compressors-part I: compression process modeling. *International Journal of Refrigeration* , *25*, 731–750. www.elsevier.com/locate/ijrefrig

Hanjalic, K., & Stosic, N. (1997). *Development and Optimization of Screw Machines With a Simulation Model-Part II: Thermodynamic Performance Simulation and Design Optimization*. http://fluidsengineering.asmedigitalcollection.asme.org.

Morishita, E., Sugihara, M., Inaba, T., Nakamura, T., Morishita, E., Sugihara, M., Inaba, T., Nakamura, T., & Works, W. (1984). Purdue e-Pubs Scroll Compressor Analytical Model SCROLL COMPRESSOR ANALYTICAL MODEL. *International Compressor Engineering Conference*. https://docs.lib.purdue.edu/icec

Read, M. G., Stosic, N., & Smith, I. K. (2019). *The influence of rotor geometry on power transfer between rotors in gerotor-type screw compressors*.

Stosic, N., & Hanjalic, K. (1997). *Development and Optimization of Screw IVIachines With a Simulation Model-Part I: Profile Generation*. http://fluidsengineering.asmedigitalcollection.asme.org.